https://doi.org/10.5194/egusphere-2024-1036
Preprint. Discussion started: 18 April 2024

Translating deposition rates into erosion rates with landscape evolution modelling

Willem Marijn van der Meij[1]

[1]Institute of Geography, University of Cologne, Zülpicher Straße 45, 50674 Cologne, Germany
Correspondence to: W. Marijn van der Meij (m.vandermeij@uni-koeln.de)

Abstract. Soil erosion is one of the main threats to agricultural food production due to the loss of fertile soil. Determination of erosion rates is essential to quantify the degree of land degradation, but it is inherently challenging to determine temporally dynamic erosion rates over agricultural time scales. Optically Stimulated Luminescence (OSL) dating can provide temporally-resolved deposition rates by determining the last moment of daylight exposure of buried colluvial deposits. However, these deposition rates may differ substantially from the actual hillslope erosion rates.

In this study, OSL-based deposition rates were converted to hillslope erosion rates through inverse modelling with soil-landscape evolution model ChronoLorica. This model integrates geochronological tracers into the simulations of soil mixing and redistribution. The model was applied to a kettle hole catchment in north-eastern Germany, which has been affected by tillage erosion over the last 5000 years. The initial shape of the landscape and the land use history are well-constrained, enabling accurate simulations of the landscape evolution that incorporate uncertainties in the model inputs.

The calibrated model reveals an increase in erosion rates of almost two orders of magnitude from pre-historic ard ploughing up to recent intensive land management. The simulated rates match well with independent age controls from the same catchment. Uncertainty in the reconstructed initial landscape and land use histories had a minor influence of 12-16% on the simulated rates. The simulations showed that the deposition rates were on average 1.5 higher than the erosion rates due to the ratio of erosional and depositional area. Recent artificial drainage and land reclamation have increased deposition rates up to five times the erosion rates, emphasizing the need of cautious interpretation of deposition rates as erosion proxies. This study demonstrates the suitability of ChronoLorica for upscaling experimental geochronological data to better understand landscape evolution in agricultural settings.

1 Introduction

Soil erosion is one of the main threats to agricultural land and food provision, because it reduces agricultural productivity by loss of fertile soil (Rhodes, 2014). Soil erosion is not only a problem of recent times. Already in the prehistoric, the first land use activities, such as deforestation and manual hoeing, triggered soil loss by removing the protective vegetative cover and loosening up the soil (Dreibrodt et al., 2010; Vanwalleghem et al., 2017). With developments in agricultural practices and an increase in food demand, agricultural activity and consequently soil erosion increased over time. In current intensively

https://doi.org/10.5194/egusphere-2024-1036
Preprint. Discussion started: 18 April 2024

managed landscapes, where land use is heavily mechanized, averaged rates of soil loss can exceed 15 t ha^{-1} a^{-1} (Nearing et al., 2017).

Prehistoric erosion rates are often magnitudes smaller than current-day erosion rates, but over the long agricultural use of many fields, may have contributed substantially to the overall land degradation. It is inherently challenging to resolve temporally dynamic erosion rates over agricultural time scales, especially in systems where erosion types and rates have changed over time (Loba et al., 2022). Geochronometers such as radionuclides can provide erosion rates that are averaged over timescales that depend on their half-lives, such as cosmogenic nuclides (Granger and Schaller, 2014), or on the moment of introduction in the landscape, such as fallout radionuclides (Mabit et al., 2008; Peñuela et al., 2023). Other geochronometers, such as radiocarbon dating or optically stimulated luminescence (OSL) dating do have the ability to provide temporally resolved rates by dating layers from different depths. However, these techniques provide deposition rates instead of erosion rates, as they rely on deposited or buried material. These deposition rates can act as proxies for erosion rates, but will also be affected by other factors, such as the ratio between erosional and depositional area, the sedimentological connectivity of the hillslope and the capacity to store sediments in depositional locations. Deposition rates can therefore deviate substantially from the actual erosion rates, which could lead to erroneous evaluation of land degradation.

In this work, deposition rates determined with OSL dating will be translated into erosion rates using inverse landscape evolution modelling. OSL dating measures the built-up luminescent signal in soil minerals (often quartz or feldspar), that accumulates due to ionizing radiation in the subsurface and incoming cosmic radiation. The luminescence signal resets when the soil particle is exposed to daylight. The luminescence is thus a proxy for the duration of burial (Murray and Roberts, 1997). Advances in numerical soil-landscape evolution models enable the tracing of geochronometers such as OSL particles and radionuclides with simulated mixing and transport processes over decadal to millennial timescale (ChronoLorica, Van der Meij et al., 2023). Through inverse modelling, hillslope erosion rates could be derived from the depositional ages determined with OSL. Such a modelling exercise requires detailed information on the major erosion processes that occur in the landscape, the initial shape of the terrain and erosion and land use history during the evolution of the landscape (Tucker and Hancock, 2010; Perron and Fagherazzi, 2012; Finke et al., 2015). These initial and boundary conditions come with uncertainty, especially when they have to be reconstructed beyond timespans where observations are available. This uncertainty should be quantified and incorporated in simulations of soil and landscape evolution to better convey our confidence in the model results (Perron and Fagherazzi, 2012; Minasny et al., 2015). Through comparison with independent data and age controls, the validity of the calibrated parameters and their uncertainty can be tested (Temme et al., 2017).

The objectives of this paper are to test 1) whether luminescence-based deposition rates can be translated into erosion rates using a soil-landscape evolution model, 2) how these rates are affected by uncertainties in initial and boundary conditions, and 3) how the reconstructed rates compare to rates derived from other geochronological methods.

https://doi.org/10.5194/egusphere-2024-1036
Preprint. Discussion started: 18 April 2024

2 Study area

The study area is the agricultural landscape laboratory CarboZALF-D (Figure 1, Sommer et al., 2016). This site is located in the young morainic landscape in northeastern Germany, which formed after the last glacial retreat in the Weichselian around 19 ka ago (Lüthgens et al., 2011). The parent material is illitic, calcareous glacial till. Annual rainfall is around 480 mm and annual mean temperature is 8.7 °C. The first agricultural practices started around ~5 ka ago, with intensification in the last 1000 years (Kappler et al., 2018; Van der Meij et al., 2019; Öttl et al., 2023).

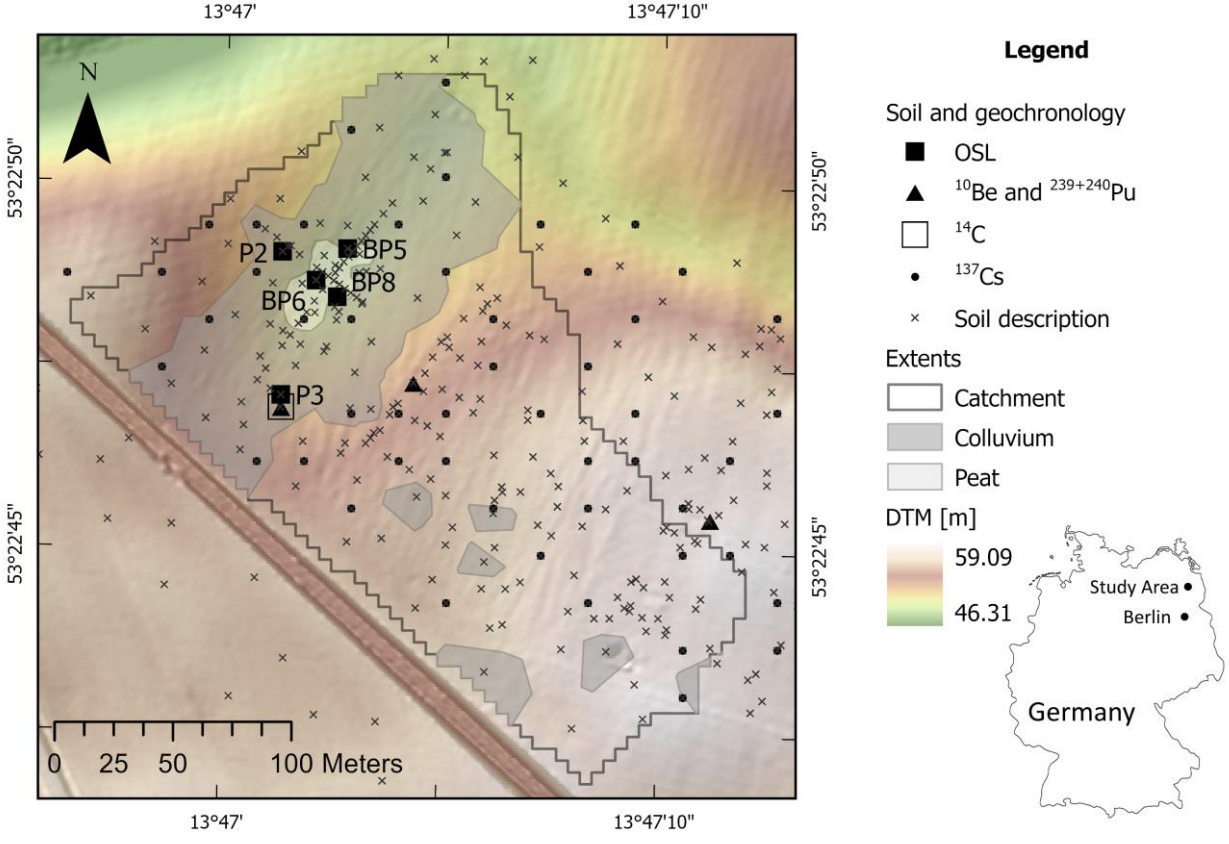

Figure 1: Map of the study area CarboZALF-D, showing the locations where the geochronological samples and soil descriptions were taken. They grey shaded areas indicate where colluvium and peat are currently present.

CarboZALF-D is a closed kettle hole catchment, meaning that almost all eroded sediments are stored in the central depression, providing unique opportunities for studying erosion processes and landscape reconstruction. This includes a reconstruction of the palaeotopography before anthropogenic erosion using truncation of soil profiles (Van der Meij et al., 2017), determination of deposition rates and patterns using optically stimulated luminescence (Van der Meij et al., 2019), determination of short-term and long-term erosion rates using $^{239+240}$Pu and meteoric and in-situ ^{10}Be (Calitri et al., 2019),

https://doi.org/10.5194/egusphere-2024-1036
Preprint. Discussion started: 18 April 2024

and determination of recent erosion rates using ^{137}Cs (Aldana Jague et al., 2016). Altogether, this resulted in a large geochronological dataset covering different spatial and temporal scales (Figure 1).

2.1 Landscape evolution at CarboZALF-D

CarboZALF-D underwent a complex landscape evolution (Van der Meij et al., 2019). Two distinct layers of colluvium could be identified. The first layer, with ages from 5 ka up to 300 a, was deposited at the fringes of the colluvium, but did not reach into the central kettle hole. This area was probably too wet for agricultural practices such as tillage, as identified by the peaty layer that is still present under the colluvium. Following drainage at the start of the 19th century to increase agricultural acreage, the central depression became accessible for agricultural practices. Continued erosion in the catchment, including re-erosion of the old colluvium, led to the deposition of a younger layer of colluvium in the central depression, covering the old colluvium at the fringes. With modernization of agricultural tools and increased tractive power, recent erosion rates far exceed the (pre-)historical erosion rates (Sommer et al., 2008). The CarboZALF-D catchment is split by a railroad constructed around 1900 CE. The southwestern part of the catchment is relatively flat and most soil profiles are still intact (Van der Meij et al., 2017). Therefore, the assumption in this paper is that that part didn't contribute substantially to the build-up of the colluvium in the central depression. It was therefore left out of the analysis.

Table 1: Overview of land management history at CarboZALF-D. Periods of different plough uses with corresponding mixing depths and their uncertainties are indicated. Modified from Van der Meij et al. (2019).

Management type	Introduction year of management type	Mixing depth (cm)	Corresponding tillage parameter
Ard plough	3700-3200 BCE	5-7	TI_{pot}_1
Medieval mouldboard plough	200-900 CE	8-15	TI_{pot}_2
Early modern mouldboard plough	1795-1800 CE	15-17	TI_{pot}_3
Contemporary mouldboard plough	1954-1965 CE	25-30	
Current mouldboard plough	1989 CE	20	
Artificial drainage	1787-1826 CE	-	-

2.2 The erosion processes

In the young morainic landscape of northeastern Germany, tillage is currently the dominant erosion process and played a substantial role in the past as well (Aldana Jague et al., 2016; Van der Meij et al., 2019; Wilken et al., 2020; Öttl et al., 2023). This is best expressed in the erosion and deposition patterns, with most intensive erosion on convex hillslopes and deposition in concave positions (De Alba et al., 2004), which are observed in current agricultural landscapes and long-term (>240 a) forested landscapes (Van der Meij et al., 2017; Calitri et al., 2020, 2021). These findings indicate that diffusive soil transport, caused by tillage erosion, has been the dominant erosion process in the study area. Therefore, and to facilitate the modelling exercise, tillage is considered the sole erosion process in this study.

https://doi.org/10.5194/egusphere-2024-1036
Preprint. Discussion started: 18 April 2024

3 Methods

3.1 ChronoLorica

3.1.1 Model architecture

Soil-landscape evolution model ChronoLorica was used for simulating the landscape evolution (Van der Meij et al., 2023; Van der Meij and Temme, 2022). ChronoLorica is based on soil-landscape evolution model Lorica (Temme and Vanwalleghem, 2016), with the addition of a geochronological module. This module couples the soil and landscape forming processes to the redistribution of different geochronometers, in this case particle ages that are analogous to OSL ages. The landscape surface is represented by a raster-based elevation model. Below each raster cell there is a pre-defined number of soil layers. Inside each layer, the model keeps track of five texture classes (gravel, sand, silt, clay, fine clay). Changes in the mass of the soil constituents due to additions or removals is converted into a change in layer thickness and consequently elevation of the surface through the bulk density. In these simulations, a constant bulk density of 1500 kg m^{-3} was used, because pedotransfer functions that are usually used to calculate the bulk density underestimate the bulk density of glacial till. A more detailed description of the model architecture can be found in Temme and Vanwalleghem (2016) and Van der Meij et al. (2023).

The three-dimensional representation of the soil landscape enables the simulation of depth functions of particle ages and radionuclides, which facilitates comparison with measured age-depth functions. This is not possible with most other landscape evolution models that only consider two-dimensional landscape surfaces.

3.1.2 Process descriptions

In ChronoLorica, tillage is simulated as a two-part process. The first part addresses the soil mixing. Over the range of the plough depth *pd* [m], soil layers are completely homogenized. This includes the mineral soil, organic components, stocks of radionuclides and particles with OSL ages.

The second part addresses soil translocation by tillage. Tillage erosion and deposition follows a linear diffusion equation (Eq. (1)). The transport of tilled material to a lower-lying neighbour (TI_{local}, [m]) is a function of the potential tillage parameter TI_{pot} [-], local slope and plough depth. TI_{pot} is distributed over all lower-lying neighbouring cells, proportional to their slopes to the power of a convergence factor p [-] (Holmgren, 1994). Then it is multiplied with the slope gradient Λ_{local} [m m^{-1}] and the plough depth.

$$TI_{local} = TI_{pot} \frac{\Lambda_{local}^{p}}{\sum_{j}^{J} \Lambda_{j}^{p}} * \Lambda_{local} * pd \quad (1)$$

This formulation was used instead of the conventional diffusion Equation from Govers et al. (1994), because it explicitly considers the effect of plough depth on tillage redistribution. In Govers et al. (1994), this is encapsulated in the tillage constant k_{til}. Both equations are equivalent and can be transformed into each other through a bulk density value.

https://doi.org/10.5194/egusphere-2024-1036
Preprint. Discussion started: 18 April 2024

ChronoLorica's particle age module keeps track of the location of a small number of OSL particles throughout the simulations. The fate of the OSL particles is coupled to the sand fraction in the model, which is the fraction that is commonly selected for OSL dating. The age of the OSL particles is increased with one for every simulation year. The age of particles present in the surficial bleaching layer of predetermined depth is reset every simulation year. The transport and bleaching of OSL particle ages are modelled as a stochastic process. The probability that a particle is transported as consequence of mixing or erosion processes is equal to the mass of transported sand [kg] divided by the total mass of sand in the source layer [kg].

3.1.3 Parametrization

The parent material of the soils was based on average parent material properties from CarboZALF-D soils (sand 53%, silt 34%, clay 13%). The initial topography was derived from reconstructions based on soil profile truncations and colluvial additions to the current landscape (reconstruction 2c, Van der Meij et al., 2017). The initial soil profiles were 2 meters deep, consisting of 40 layers of 5 cm. The amount of OSL particles was set to ~150 grains per layer and the bleaching depth was set to 5 mm. Simulations were 5000 years, through which plough depth and tillage intensity changed based on values in Table 1 and the calibrated tillage intensities (Section 3.2). To mimic the two-stage landscape evolution at CarboZALF-D, the central kettle hole, with the size of the current peat extent, was only included in the last ~200 years, following the artificial drainage. Model output was provided every 100 years during most of the simulations and every 10 years after the artificial drainage.

3.2 Inverse modelling

The unknown parameter in the tillage equation (Eq. (1)) is the potential tillage parameter TI_{pot}. This parameter was calibrated using the OSL dates from Van der Meij et al. (2019) through inverse modelling. These OSL samples were taken from five different locations in the colluvial depression (Figure 1). Samples taken from the soil buried below the colluvium and from the plough layer were excluded, leaving 27 OSL samples. To account for changes in TI_{pot} in time, the periods of different management types were aggregated to three periods with each their own potential (but unknown) tillage rate (Table 1). For each period, the average introduction year and plough depth were used in the inverse modelling (Figure 2). The first period is the ard plough period, from the start of the simulations (3000 BCE) until 550 CE, with seven OSL dates covering this timeframe. The second period is the Medieval mouldboard plough, lasting until 1800 CE. There are no OSL dates that fall in this period, probably because sediments from this period located on the fringes of the depression have been re-eroded when the central depression was reclaimed. It was still possible to calibrate a TI_{pot} for this period based on the total amount of sediments that was required for filling the central depression without eroding the fringes beyond where the OSL dates from period 1 were located. The final period lasted until the end of the simulations and represents the use of the modern mouldboard plough. For this period there were 20 OSL dates.

https://doi.org/10.5194/egusphere-2024-1036
Preprint. Discussion started: 18 April 2024

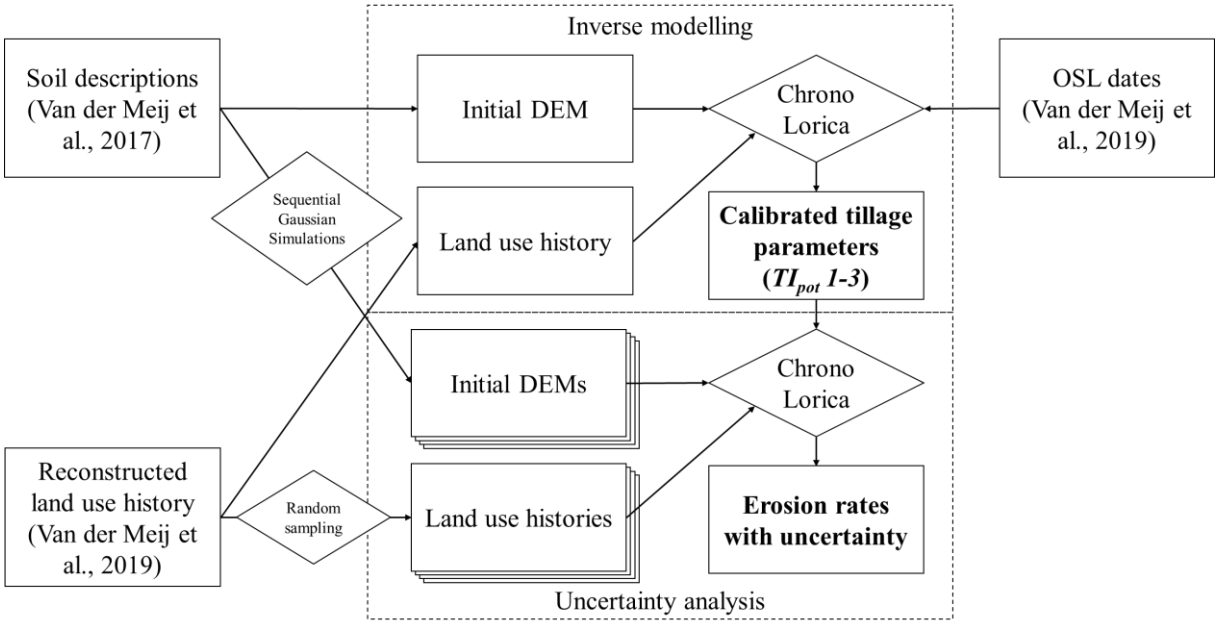

Figure 2: Workflow for the inverse modelling and uncertainty analysis in this study.

For each OSL sample, the equivalent layer at the same location and same depth in the simulated soil landscape was identified and the mode of its age distribution was derived. For samples for which there was no equivalent layer, for example due to too thinly simulated colluvium, a dummy age of two times the simulation time was used to ensure that such an error was penalized heavily. The three TI_{pot}s were calibrated by minimizing the absolute difference between the modes of the measured and simulated age distributions.

3.3 Uncertainty from initial and boundary conditions

The initial and boundary conditions come with uncertainties, as is evidenced by the interpolation uncertainty of interpolated soil and colluvium thickness reported in Van der Meij et al. (2017) and the ranges of introduction years and plough depths in Table 1. This uncertainty was accounted for in the reconstruction of erosion rates by doing a sensitivity analysis after the model calibration (Figure 2). For the initial topography, 10 realizations of interpolated soil and colluvium thickness were made using Sequential Gaussian Simulation with the gstat package version 2.1-1 (Pebesma and Gräler, 2023), which randomly samples unique initial landscapes within the interpolation uncertainty. For the boundary conditions, 20 land use histories with corresponding plough depths were randomly sampled from the values in Table 1, assuming uniform distributions for each range of values. The combination of the different initial topographies and land use histories produced 200 unique model runs, from which the average and 2-sigma error ranges of rates of landscape change are presented in the remainder of this paper.

https://doi.org/10.5194/egusphere-2024-1036
Preprint. Discussion started: 18 April 2024

3.4 Evaluation

The simulated topographical changes and erosion and deposition rates from ChronoLorica were evaluated with different geochronological and erosion datasets. The simulated spatial patterns of erosion and deposition in the calibrated model run were compared with reconstructed elevation changes from Van der Meij et al. (2017). The simulated erosion and deposition rates resulting from the sensitivity analysis were compared with rates derived from OSL, ^{10}Be, ^{137}Cs, $^{239+240}$Pu and ^{14}C data (Aldana Jague et al., 2016; Calitri et al., 2019; Van der Meij et al., 2019).

4 Results

4.1 Model calibration

Figure 3 shows the measured and calibrated age-depth profiles for all sampling locations. The calibrated depth-profiles follow the measured profiles, although some profiles are overall younger than simulated (P3, BP5), whereas other profiles are overall older than simulated (BP8). The thickness of the colluvium is simulated thinner than observed for the fringe positions P2 and P3, while it is simulated similar or thicker for the locations in the central depression.

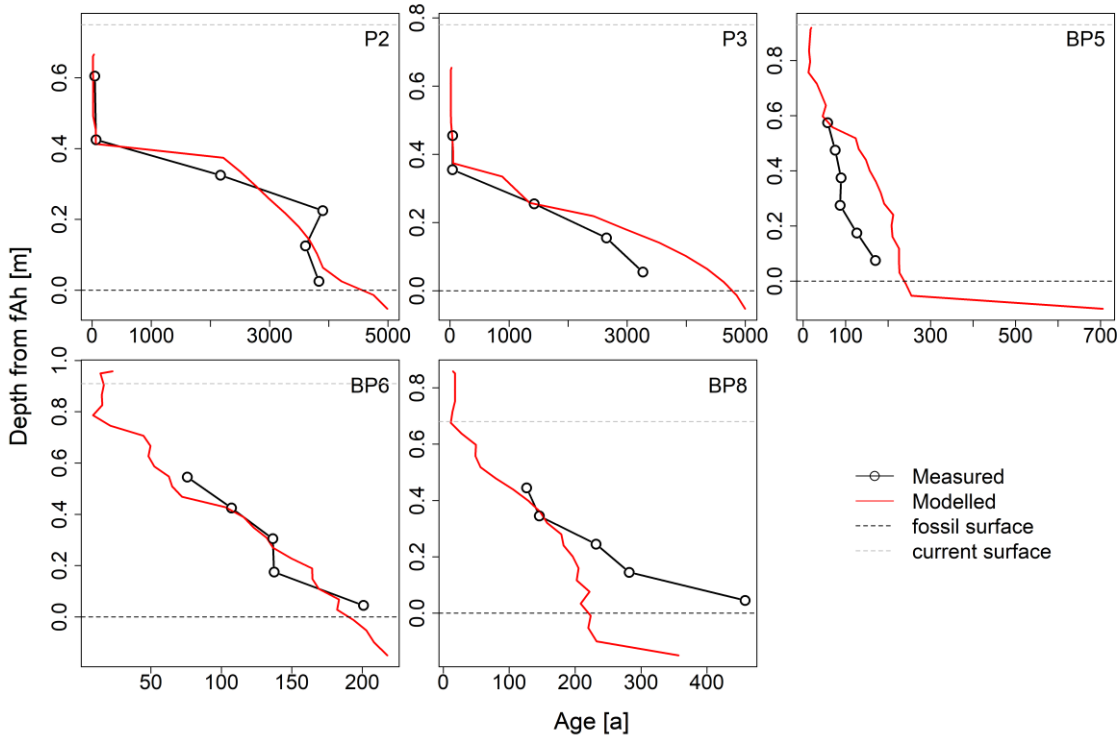

Figure 3: Depth plots showing the modes of the measured and simulated ages of the calibration run with the lowest error. The horizontal dashed lines indicate the observed levels of the fossil surface below the colluvium and the current soil surface.

https://doi.org/10.5194/egusphere-2024-1036
Preprint. Discussion started: 18 April 2024

The calibrated tillage parameters show an increase through time and thus agricultural intensification, with 0.13 for the period of the ard plough, 0.16 for the period of the Medieval mouldboard plough and 0.38 for the period of the modern mouldboard plough. When including the differences in ploughing depth in these periods (Table 1), which also affect tillage erosion rates (Eq. (1)), the intensity of tillage erosion and deposition for both historical periods were 8% and 19% of the contemporary tillage intensity.

Since OSL particle tracing operates as a stochastic process, the distribution and ages of particles will be different between runs. To assess the impact of this on the calibration, a simulation was repeatedly performed with the same parameter set. This resulted in a relative error of 0.2% in the calibration error, and had no discernible effect on the overall calibration outcomes.

4.2 Reconstructed and simulated elevation changes

The simulated elevation changes with ChronoLorica resemble the reconstructed elevation changes by Van der Meij et al. (2017) (Figure 4A, B). The extent of the central colluvium is smaller in the simulated elevation changes, while the size of depositional areas on the hillslope is slightly larger. The differences between the reconstructed and simulated elevation changes (Figure 4C) indicate that the simulations predicted slightly more erosion (mean error (ME) = 0.03 m), less deposition (ME = -0.15 m), and overall less elevation change in the catchment (ME = -0.04 m compared to the reconstructions.

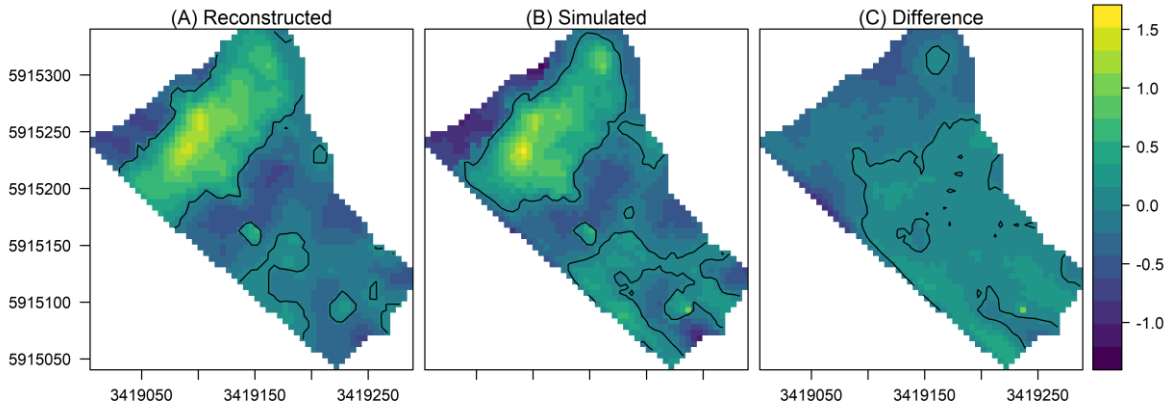

Figure 4: Elevation changes derived from A) reconstructions with field data (Van der Meij et al., 2017), B) the calibrated simulations and C) the difference between both maps (simulated minus reconstructed). Contour lines indicate elevation differences of 0 m.

4.3 Erosion and deposition rates

The simulated erosion and deposition rates vary by two orders of magnitude over time (Figure 5A). The catchment-averaged rates (dashed lines) show the same trend as the 95th percentile of elevation change (solid lines), but are on average 3-4 times

https://doi.org/10.5194/egusphere-2024-1036
Preprint. Discussion started: 18 April 2024

lower. Both erosion and deposition rates start relatively high at the start of the simulations and drop an order of magnitude during the period of ard ploughing. The transition to the period of the Medieval mouldboard plough shows an increase of the rates. The rates in the period of the modern mouldboard plough are again much higher, ranging up to 1 cm per year for the 95th percentile of the simulated rates. The uncertainty of the erosion and deposition rates is relatively constant through time, except during the switch from one plough regime to the next, which is especially evident for the uncertain transition from ard to Medieval mouldboard period. The simulated variation in erosion rates is 12-16% due to uncertain initial and boundary conditions. Uncertainties from these sources contribute in almost equal amounts to the overall uncertainty in rates of landscape change, but do show different temporal patterns (Figure 5B). Uncertainty derived from the initial conditions is highest at the start and diminishes throughout the simulations as the tillage process smoothes different landscapes to similar end products. Uncertainties from boundary conditions start at lower levels and diminish throughout a ploughing period, but increase again during shifts in management regime.

Rates derived from the experimental geochronological data follow the same trends as the simulated rates. In-situ and meteoric ^{10}Be show rates in and below the lower regions of the simulation. The catchment-averaged rates derived with ^{137}Cs is in the same order of magnitude as recent simulated catchment-averaged erosion and deposition rates. Rates derived with OSL and $^{239+240}$Pu lean towards the higher end of the simulated rates.

With the exception of the first ~1000 years, catchment-averaged deposition rates are 1-1.5 times higher than erosion rates (Figure 5C). In the last ~220 years, following the drainage and cultivation of the central depression, deposition rates were up to five times as high as the erosion rates.

https://doi.org/10.5194/egusphere-2024-1036
Preprint. Discussion started: 18 April 2024

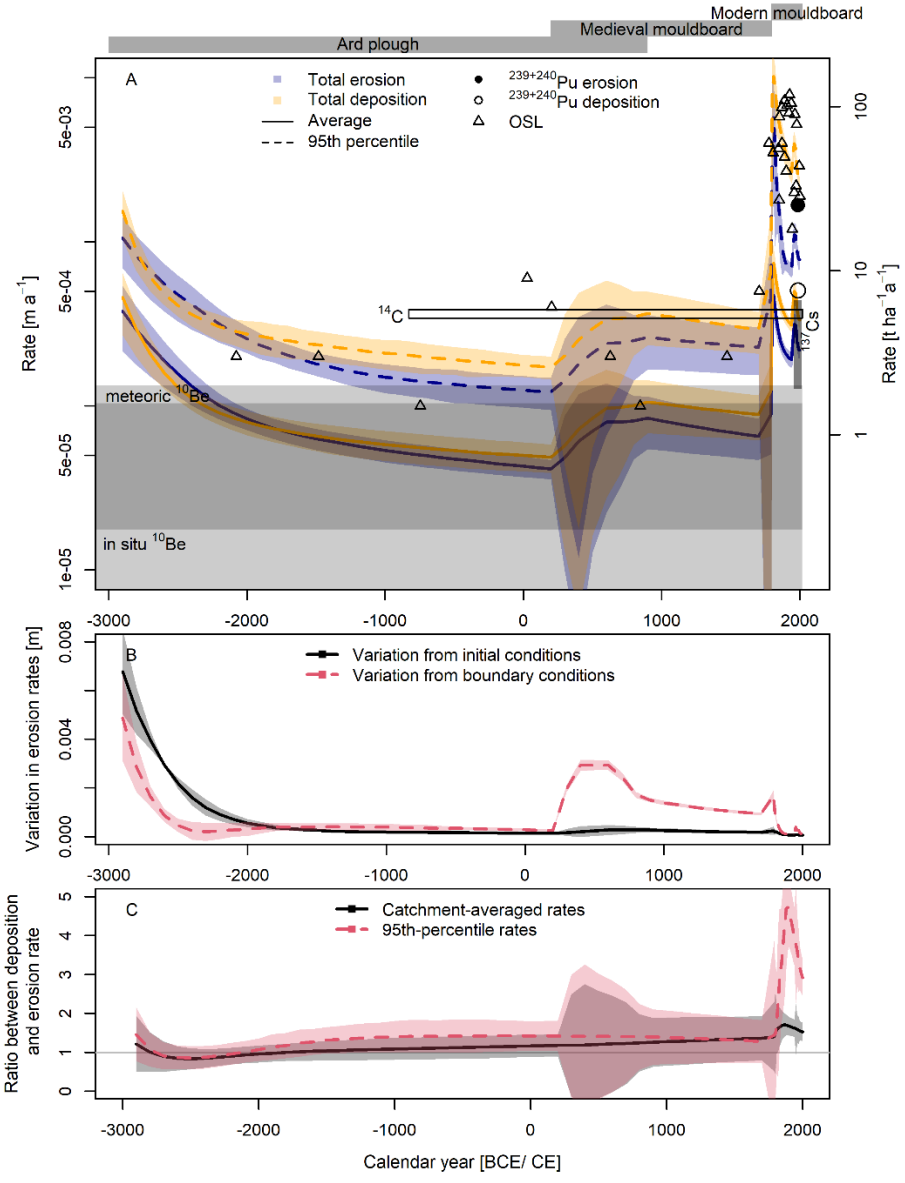

Figure 5: A) Compilation of simulated and measured erosion and deposition rates. Simulated rates are provided in the blue [erosion] and orange [deposition] bands and lines, for the catchment-averaged rates (dashed lines) and the 95th percentile of erosion and deposition rates to represent severe erosion and deposition locations (solid lines). Experimental data is provided with either rectangles representing their representative periods and corresponding rates with uncertainty, or as point information. Closed rectangles and symbols represent erosion rates, while open rectangles and symbols represent deposition rates. All provided uncertainties are 2-sigma intervals, except for ^{137}Cs (80% interval). For $^{239+240}$Pu and OSL, uncertainties are not provided, because they are not provided or they obscure the rest of the Figure. B) Variation in erosion rates coming from uncertainties in initial conditions and boundary conditions, expressed as the standard deviation in catchment-averaged erosion rates. C) Ratio between deposition and erosion rates, for catchment-averaged and 95th-percentile rates, provided with mean and 2-sigma uncertainty. Numbers larger than 1 indicate higher deposition rates.

https://doi.org/10.5194/egusphere-2024-1036
Preprint. Discussion started: 18 April 2024

5 Discussion

5.1 Calibration on spatial data

The OSL data gathered from five locations in the depression were used to calibrate temporally varying potential tillage constants (Figure 3). The measured and modelled age-depth plots are not identical, but do follow the same trends and have ages in the same ranges. While calibration using data from a single location might yield a more precise calibration line, it would be based on a smaller dataset and overlook spatial variations in the deposition process. Utilizing spatial calibration data provided a sufficient number of calibration points for the calibration of the tillage constants while also considering spatial patterns of deposition, which are complex for this kettle hole catchment (Van der Meij et al., 2019).

The match between simulated and reconstructed elevation changes indicates that the calibrated model simulates the landscape evolution fairly well (Figure 4). The small overestimation of erosion and larger underestimation of deposition indicate a possible unconsidered source of sediments in the depression, such as a part of the catchment located beyond the railroad track. However, this discrepancy can also be a result of uncertainties in the reconstruction of elevation changes and the simulations. When considering root mean squared errors (RMSE) of reconstructed versus simulated elevation changes, the run with calibrated potential tillage parameters of 0.14 and 0.4 for periods 2 and 3 would yield the lowest error. These values are consistent with the calibrated parameters using the OSL datings (0.13 and 0.38 respectively), and provide another line of evidence for the plausibility of the calibrated parameters.

TI_{pot} functions in the same fashion as the parameter B in the Equation of the tillage constant k_{til} from Govers et al. (1994). Through the bulk density and plough depth, the calibrated TI_{pot} can be converted to k_{til}. Öttl et al. (2023) made an extensive compilation of experimental k_{til} values from different machineries and plough types and placed them along a timeline of agricultural use over the last 1000 years for the region around CarboZALF-D. The values from this study fall in the lower range of the compiled values, and the value for the ard plough (11.7 kg m^{-1}) is even under the lowest reported value. This could be explained by much less intense land reworking in the prehistoric times than in more recent uses of the ard plough. The value for the Medieval mouldboard period (27.6 kg m^{-1}) is above the lowest reported values for the first reported mouldboard uses. Calibration of this period was complicated due to the lack of OSL dates falling in this time period, and therefore the calibrated parameter should be considered with care. The values for the modern mouldboard plough match better with the compilation of tillage constants, where the values for the period around 1800 (91.2 kg m^{-1}) is similar to the median reported value and the value for the recent period with heavy machinery (156.8 kg m^{-1}) is above the 25th percentile. Overall, the calibrated values for the last 200 years match well with the compilation of Öttl et al. (2023) and provide local estimates for tillage constants for future tillage erosion studies.

5.2 Effect of uncertainties

Uncertainty in reconstructed initial and boundary conditions and model formulation will propagate through the model simulations and affect the accuracy of the model outcomes (Perron and Fagherazzi, 2012; Temme et al., 2017). This

https://doi.org/10.5194/egusphere-2024-1036
Preprint. Discussion started: 18 April 2024

uncertainty propagation is often neglected due to limited information on the level of uncertainty associated with the model inputs. The CarboZALF-D area provides a unique setting for assessing the effects of uncertain initial and boundary conditions on model output, as these initial and boundary conditions including uncertainty are well-constrained, the landscape evolution is complex but only subject to one main process and there is independent data for verifying the calculated erosion and deposition rates. The relative standard deviations of the simulated erosion and deposition rates range between 12 and 16%. Variations in initial and boundary conditions contribute in equal amounts to the overall uncertainty in erosion rates in the catchment, but do so show different temporal patterns (Figure 5B). The effect of uncertainty in the initial landscape on the variation in erosion rates is mainly visible at the start of the simulations, after which it diminishes to a steady low level. Uncertainty in the boundary conditions affects variation in erosion rates at the start of the simulations and after shifts in plough regime. This suggests that, over the entire simulation period, the overall landscape change is only affected to a small degree by the uncertainty in the inputs.

These simulations did not consider uncertainties in model parameters, although these also can affect model outputs (Skinner et al., 2018). The uncertainty in the tillage parameters could potentially be quantified by considering uncertainty in initial and boundary conditions during the calibration, but this would require an unrealistic number of simulations and runtime. This study required about 160 model runs for the full calibration using fixed initial and boundary conditions, each run taking approximately three hours. Considering the uncertainties in the inputs would require 200 times more simulations, corresponding to ~11 CPU years at the time of writing.

5.3 Comparison of erosion and deposition rates

The inverse modelling provided spatial and temporal variations in erosion rates, based on the deposition rates derived from OSL dating (Figure 5A). Pre-industrial catchment-averaged erosion rates were in the order of 1 t ha^{-1} a^{-1}, resembling natural soil production rates and erosion rates under present-day conservation agriculture and exceed erosion rates under natural vegetation (Alewell et al., 2015; Minasny et al., 2015; Nearing et al., 2017). Erosion rates under the modern mouldboard plough are almost an order of magnitude higher (5-10 t ha^{-1} a^{-1}), with local extreme erosion rates ranging up to 100 t ha^{-1} a^{-1}. These rates are consistent with erosion rates under conventional agriculture (Minasny et al., 2015; Nearing et al., 2017).

The simulated erosion and deposition rates match well with the independent age controls. The rates estimated with in-situ and cosmogenic ^{10}Be are on the lower range of the simulated values or even below, but these represent average erosion rates over the entire age of the area of ~19ka (Lüthgens et al., 2011; Calitri et al., 2019; Loba et al., 2022) and are therefore expected to be lower than the simulated agricultural erosion rates in the last 5000 years. The radiocarbon age and OSL ages all match with the higher estimates of deposition rates, both in the past as in more recent times (Calitri et al., 2019; Van der Meij et al., 2019). Erosion rates derived from $^{239+240}Pu$ are higher than recent simulated erosion, while deposition rates determined with $^{239+240}Pu$ match the high deposition rates very well. The catchment-averaged erosion rates determined with ^{137}Cs fits very well with the simulated recent catchment-averaged erosion rates (Aldana Jague et al., 2016). All these lines of

https://doi.org/10.5194/egusphere-2024-1036
Preprint. Discussion started: 18 April 2024

evidence indicate that the simulations resulted in plausible erosion and sedimentation rates that represent landscape evolution under different types of land management and over different timescales.

The deposition rates are almost always higher than the erosion rates (Figure 5C), which confirms the hypothesis that the deposition rates cannot be used as proxies for erosion rates. In the period up to the artificial drainage, the ratio of deposition rates and erosion rates of ~1.5 m m^{-1} reflects the ratio between the size of the erosional and depositional areas on the hillslope. This makes sense from a mass balance perspective, because the eroded material all accumulates in the depositional area in this catchments (Van der Meij et al., 2017). The artificial drainage increased the size of the depositional area by a small amount, but the deposition-erosion rate did not decrease in a similar manner, but instead increased up to 5 m m^{-1}. The large increase in gradients towards the centre of the depression triggered re-erosion of the previously deposited material on the fringes of the depression and resulted in very high deposition rates in the previously un-cultivated centre, shifting the balance between erosion and deposition rates.

These findings indicate that indeed deposition rates do not represent hillslope erosion rates. Ratios between eroding and depositional areas could be used to recalculate erosion rates into deposition rates, but special attention should be given to other environmental factors that could affect the balance of these rates. These factors include changes in land management, shifts in erosion and deposition patterns, and the balance between sediment storage within the catchment and exported sediment, a common consideration for most other catchments.

5.4 Combining geochronometers with landscape evolution models

In this study, deposition rates were recalculated into soil erosion rates using a soil-landscape evolution models and the results were verified with independent radio-nuclide based geochronometers (Figure 5A). Radionuclides are commonly used to study soil erosion over decadal to millennial timescales, often in combination with soil erosion or landscape evolution models (Van Oost et al., 2003; Yang et al., 2006; Wilken et al., 2020). However, these only provide a temporally-averaged erosion rate, depending on their half-life or moment of introduction. This especially complicates their application in systems with changing erosion rates over time, for example due to changing tillage systems (Loba et al., 2022). A combination of different radionuclides (Mabit et al., 2008; Mudd, 2017; Hippe et al., 2021), or a combination with OSL or radiocarbon dating (Van der Meij et al., 2019) could provide additional, time-resolved, erosion and deposition rates to further distinguish temporal changes in the erosion history of transient agricultural landscapes. Models such as ChronoLorica are ideal tools to combine these different geochronometers into a coherent landscape evolution framework and to fill in the gaps in the erosion rates, in both spatial and temporal dimensions.

6 Conclusions

This study presents a modelling exercise where OSL-based deposition rates were successfully recalculated into hillslope erosion rates using inverse modelling with soil-landscape evolution model ChronoLorica. The kettle hole catchment

https://doi.org/10.5194/egusphere-2024-1036
Preprint. Discussion started: 18 April 2024

CarboZALF-D in northeastern Germany provided an ideal test area for this, due to the well-constrained initial shape of the landscape and reconstructions of plough uses through time, including their uncertainties, and other geochronological datasets that could be used for independent validation.

The erosion rates increased almost two orders of magnitude from pre-historic ard ploughing up to recent intensive land management. The uncertainties in initial and boundary conditions only affected the simulations in a minor way, with 12-16% relative error in the simulated erosion and deposition rates. The simulated rates match well with the independent age controls and values reported in literature. The deposition rates were on average 1.5 times higher than erosion rates, reflecting the ratio between eroded and depositional area. Due to artificial drainage in recent times and an increase in erosional gradients, deposition rates were up to five times as high as the erosion rates, indicating that deposition rates cannot be used as direct proxies of erosion rates and that catchment construction and changes in land management should be considered here as well.

ChronoLorica proves to be an ideal modelling tool for studying landscape evolution in small catchments. Through calibration with field and experimental data, landscape processes and rates can be upscaled and better understood. The model can integrate different geochronometers into a coherent framework of landscape evolution, suitable for resolving temporally varying erosion and deposition rates.

Code and data availability

The ChronoLorica model is publicly available via https://doi.org/10.5281/zenodo.7875033 (Van der Meij and Temme, 2022). The maintained versions of ChronoLorica and other versions of the Lorica model are accessible through https://github.com/arnaudtemme/lorica_all_versions (last access: 3 April 2024).

The OSL data used in this study is published in earlier work (Van der Meij et al., 2019) and available upon request from the corresponding author.

Competing interests

The author declares that he has no conflict of interest.

Acknowledgments

I thank Arnaud Temme for fruitful discussions regarding the modelling and for proofreading the manuscript.

https://doi.org/10.5194/egusphere-2024-1036
Preprint. Discussion started: 18 April 2024

References

Aldana Jague, E., Sommer, M., Saby, N. P. A., Cornelis, J.-T., Van Wesemael, B., and Van Oost, K.: High resolution characterization of the soil organic carbon depth profile in a soil landscape affected by erosion, Soil and Tillage Research, 156, 185–193, https://doi.org/10.1016/j.still.2015.05.014, 2016.

Alewell, C., Egli, M., and Meusburger, K.: An attempt to estimate tolerable soil erosion rates by matching soil formation with denudation in Alpine grasslands, Journal of Soils and Sediments, 15, 1383–1399, https://doi.org/10.1007/s11368-014-0920-6, 2015.

Calitri, F., Sommer, M., Norton, K., Temme, A., Brandová, D., Portes, R., Christl, M., Ketterer, M. E., and Egli, M.: Tracing the temporal evolution of soil redistribution rates in an agricultural landscape using 239+240Pu and 10Be, Earth Surface Processes and Landforms, 44, 1783–1798, https://doi.org/10.1002/esp.4612, 2019.

Calitri, F., Sommer, M., Van der Meij, W. M., and Egli, M.: Soil erosion along a transect in a forested catchment: Recent or ancient processes?, Catena, 194, 104683, https://doi.org/10.1016/j.catena.2020.104683, 2020.

Calitri, F., Sommer, M., van der Meij, W. M., Tikhomirov, D., Christl, M., and Egli, M.: 10Be and 14C data provide insight on soil mass redistribution along gentle slopes and reveal ancient human impact, J Soils Sediments, https://doi.org/10.1007/s11368-021-03041-7, 2021.

De Alba, S., Lindstrom, M., Schumacher, T. E., and Malo, D. D.: Soil landscape evolution due to soil redistribution by tillage: a new conceptual model of soil catena evolution in agricultural landscapes, CATENA, 58, 77–100, https://doi.org/10.1016/j.catena.2003.12.004, 2004.

Dreibrodt, S., Lubos, C., Terhorst, B., Damm, B., and Bork, H. R.: Historical soil erosion by water in Germany: Scales and archives, chronology, research perspectives, Quaternary International, 222, 80–95, https://doi.org/10.1016/j.quaint.2009.06.014, 2010.

Finke, P. A., Samouëlian, A., Suarez-Bonnet, M., Laroche, B., and Cornu, S. S.: Assessing the usage potential of SoilGen2 to predict clay translocation under forest and agricultural land uses, European Journal of Soil Science, 66, 194–205, https://doi.org/10.1111/ejss.12190, 2015.

Govers, G., Vandaele, K., Desmet, P., Poesen, J., and Bunte, K.: The role of tillage in soil redistribution on hillslopes, European Journal of Soil Science, 45, 469–478, https://doi.org/10.1111/j.1365-2389.1994.tb00532.x, 1994.

Granger, D. E. and Schaller, M.: Cosmogenic Nuclides and Erosion at the Watershed Scale, Elements, 10, 369–373, https://doi.org/10.2113/gselements.10.5.369, 2014.

Hippe, K., Jansen, J. D., Skov, D. S., Lupker, M., Ivy-Ochs, S., Kober, F., Zeilinger, G., Capriles, J. M., Christl, M., Maden, C., Vockenhuber, C., and Egholm, D. L.: Cosmogenic in situ 14C-10Be reveals abrupt Late Holocene soil loss in the Andean Altiplano, Nat Commun, 12, 2546, https://doi.org/10.1038/s41467-021-22825-6, 2021.

Holmgren, P.: Multiple flow direction algorithms for runoff modelling in grid based elevation models: An empirical evaluation, Hydrological Processes, 8, 327–334, https://doi.org/10.1002/hyp.3360080405, 1994.

Kappler, C., Kaiser, K., Tanski, P., Klos, F., Fülling, A., Mrotzek, A., Sommer, M., and Bens, O.: Stratigraphy and age of colluvial deposits indicating Late Holocene soil erosion in northeastern Germany, CATENA, 170, 224–245, https://doi.org/10.1016/j.catena.2018.06.010, 2018.

Loba, A., Waroszewski, J., Sykuła, M., Kabala, C., and Egli, M.: Meteoric 10Be, 137Cs and 239+240Pu as Tracers of Long- and Medium-Term Soil Erosion—A Review, Minerals, 12, 359, https://doi.org/10.3390/min12030359, 2022.

Lüthgens, C., Böse, M., and Preusser, F.: Age of the Pomeranian ice-marginal position in northeastern Germany determined by Optically Stimulated Luminescence (OSL) dating of glaciofluvial sediments, Boreas, 40, 598–615, https://doi.org/10.1111/j.1502-3885.2011.00211.x, 2011.

Mabit, L., Benmansour, M., and Walling, D. E.: Comparative advantages and limitations of the fallout radionuclides 137Cs, 210Pbex and 7Be for assessing soil erosion and sedimentation, Journal of Environmental Radioactivity, 99, 1799–1807, https://doi.org/10.1016/j.jenvrad.2008.08.009, 2008.

Minasny, B., Finke, P., Stockmann, U., Vanwalleghem, T., and McBratney, A. B.: Resolving the integral connection between pedogenesis and landscape evolution, Earth-Science Reviews, 150, 102–120, https://doi.org/10.1016/j.earscirev.2015.07.004, 2015.

Mudd, S. M.: Detection of transience in eroding landscapes, Earth Surface Processes and Landforms, 42, 24–41, https://doi.org/10.1002/esp.3923, 2017.

Murray, A. S. and Roberts, R. G.: Determining the burial time of single grains of quartz using optically stimulated luminescence, Earth and Planetary Science Letters, 152, 163–180, https://doi.org/10.1016/S0012-821X(97)00150-7, 1997.

Nearing, M. A., Xie, Y., Liu, B., and Ye, Y.: Natural and anthropogenic rates of soil erosion, International Soil and Water Conservation Research, 5, 77–84, https://doi.org/10.1016/j.iswcr.2017.04.001, 2017.

Öttl, L. K., Wilken, F., Juřicová, A., Batista, P. V. G., and Fiener, P.: A millennium of arable land use - the long-term impact of water and tillage erosion on landscape-scale carbon dynamics, EGUsphere, 1–36, https://doi.org/10.5194/egusphere-2023-1400, 2023.

Pebesma, E. and Gräler, B.: gstat: Spatial and Spatio-Temporal Geostatistical Modelling, Prediction and Simulation, 2023.

Peñuela, A., Hurtado, S., García-Gamero, V., Mas, J. L., Ketterer, M. E., Vanwalleghem, T., and Gómez, J. A.: A comparison of 210Pbxs, 137Cs, and Pu isotopes as proxies of soil redistribution in South Spain under severe erosion conditions, J Soils Sediments, 23, 3326–3344, https://doi.org/10.1007/s11368-023-03560-5, 2023.

Perron, J. T. and Fagherazzi, S.: The legacy of initial conditions in landscape evolution, Earth Surface Processes and Landforms, 37, 52–63, https://doi.org/10.1002/esp.2205, 2012.

Rhodes, C. J.: Soil Erosion, Climate Change and Global Food Security: Challenges and Strategies, Science Progress, 97, 97–153, https://doi.org/10.3184/003685014X13994567941465, 2014.

Skinner, C. J., Coulthard, T. J., Schwanghart, W., Van De Wiel, M. J., and Hancock, G.: Global sensitivity analysis of parameter uncertainty in landscape evolution models, Geoscientific Model Development, 11, 4873–4888, https://doi.org/10.5194/gmd-11-4873-2018, 2018.

Sommer, M., Gerke, H. H., and Deumlich, D.: Modelling soil landscape genesis — A “time split” approach for hummocky agricultural landscapes, Geoderma, 145, 480–493, https://doi.org/10.1016/j.geoderma.2008.01.012, 2008.

Sommer, M., Augustin, J., and Kleber, M.: Feedbacks of soil erosion on SOC patterns and carbon dynamics in agricultural landscapes—The CarboZALF experiment, Soil & Tillage Research, 156, 182–184, https://doi.org/10.1016/j.still.2015.09.015, 2016.

https://doi.org/10.5194/egusphere-2024-1036
Preprint. Discussion started: 18 April 2024

Temme, A. J. A. M. and Vanwalleghem, T.: LORICA – A new model for linking landscape and soil profile evolution: development and sensitivity analysis, Computers & Geosciences, 90, 131–143, https://doi.org/10.1016/j.cageo.2015.08.004, 2016.

Temme, A. J. A. M., Armitage, J., Attal, M., Gorp, W. van, Coulthard, T. J., and Schoorl, J. M.: Developing, choosing and using landscape evolution models to inform field-based landscape reconstruction studies, Earth Surface Processes and Landforms, 42, 2167–2183, https://doi.org/10.1002/esp.4162, 2017.

Tucker, G. E. and Hancock, G. R.: Modelling landscape evolution, Earth Surface Processes and Landforms, 35, 28–50, https://doi.org/10.1002/esp.1952, 2010.

Van der Meij, W. M. and Temme, A. J. A. M.: ChronoLorica v1.0, Zenodo [code], https://doi.org/10.5281/zenodo.7875033, 2022.

Van der Meij, W. M., Temme, A. J. A. M., Wallinga, J., Hierold, W., and Sommer, M.: Topography reconstruction of eroding landscapes–A case study from a hummocky ground moraine (CarboZALF-D), Geomorphology, 295, 758–772, https://doi.org/10.1016/j.geomorph.2017.08.015, 2017.

Van der Meij, W. M., Reimann, T., Vornehm, V. K., Temme, A. J. A. M., Wallinga, J., van Beek, R., and Sommer, M.: Reconstructing rates and patterns of colluvial soil redistribution in agrarian (hummocky) landscapes, Earth Surface Processes and Landforms, 44, 2408–2422, https://doi.org/10.1002/esp.4671, 2019.

Van der Meij, W. M., Temme, A. J. A. M., Binnie, S. A., and Reimann, T.: ChronoLorica: introduction of a soil–landscape evolution model combined with geochronometers, Geochronology, 5, 241–261, https://doi.org/10.5194/gchron-5-241-2023, 2023.

Van Oost, K., Govers, G., and Van Muysen, W.: A process-based conversion model for caesium-137 derived erosion rates on agricultural land: an integrated spatial approach, Earth Surface Processes and Landforms, 28, 187–207, https://doi.org/10.1002/esp.446, 2003.

Vanwalleghem, T., Gómez, J. A., Infante Amate, J., González de Molina, M., Vanderlinden, K., Guzmán, G., Laguna, A., and Giráldez, J. V.: Impact of historical land use and soil management change on soil erosion and agricultural sustainability during the Anthropocene, Anthropocene, 17, 13–29, https://doi.org/10.1016/j.ancene.2017.01.002, 2017.

Wilken, F., Ketterer, M., Koszinski, S., Sommer, M., and Fiener, P.: Understanding the role of water and tillage erosion from $^{239+240}$Pu tracer measurements using inverse modelling, SOIL, 6, 549–564, https://doi.org/10.5194/soil-6-549-2020, 2020.

Yang, M.-Y., Tian, J.-L., and Liu, P.-L.: Investigating the spatial distribution of soil erosion and deposition in a small catchment on the Loess Plateau of China, using 137Cs, Soil and Tillage Research, 87, 186–193, https://doi.org/10.1016/j.still.2005.03.010, 2006.